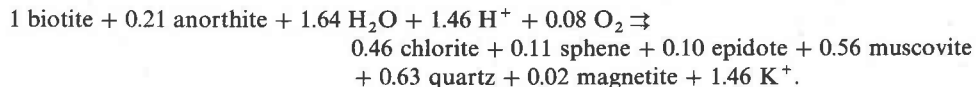# The alteration of granitic biotite to chlorite

RICHARD A. EGGLETON AND JILLIAN F. BANFIELD

*Department of Geology
Australian National University
Canberra, Australia 2601*

Abstract

Granitic biotite from southeastern Australia alters to a mixture of chlorite (65%), sphene (10%) and epidote (10%) through a hydrothermal (330–340°C) reaction in which two layers of biotite become one layer of chlorite. Loss of K from the interlayer and subsequent stripping of tetrahedral sheets from half the biotite 2:1 layers at random, as well as growth of extra brucite-like sheets between the talc-like layers of biotite, produced chlorite, resulting in a volume loss of 35%. The spaces are filled by the other reaction products and probably also by quartz. Less than 5% of the replaced biotite becomes void space. In terms of unit cells, the reaction, which is coupled to the alteration of plagioclase to sericite, can be written:

$$1 \text{ biotite} + 0.21 \text{ anorthite} + 1.64 \text{ H}_2\text{O} + 1.46 \text{ H}^+ + 0.08 \text{ O}_2 \rightrightarrows$$
$$0.46 \text{ chlorite} + 0.11 \text{ sphene} + 0.10 \text{ epidote} + 0.56 \text{ muscovite}$$
$$+ 0.63 \text{ quartz} + 0.02 \text{ magnetite} + 1.46 \text{ K}^+.$$

The tetrahedral sheet of the biotite is inherited intact by the chlorite, whereas the octahedral sheet undergoes element redistribution, primarily loss of Ti and gain of Al. The overall reaction conserves Mg in the chlorite, and Ti + Fe + Al within the pseudomorphing chlorite–sphene–epidote assemblage.

Introduction

Recent studies of the alteration of rock-forming silicates by hydrothermal, deuteric, or weathering processes appear to indicate that structural elements from the primary mineral may be inherited by the clay mineral product (Veblen and Buseck, 1980; Eggleton and Boland, 1982; Eggleton, 1983). It has been long assumed that when layer-silicates alter to clays, much of the parent mineral structure is taken over by the clay (e.g., Loughnan, 1969, p. 31). As part of a continuing project on silicate alteration, we have examined the formation of chlorite from a granitic biotite.

Parry and Downey (1982) describe hydrothermal alteration of biotite to chlorite in a quartz monzonite. They consider both isovolumetric and Al-conservative reactions, and conclude the process conserves Al and requires variable additions or subtractions of K, Mg, Fe and H. Ferry (1979) found that in an assumed Al-conservative alteration of granitic biotite to chlorite there was a 13% volume decrease, and that Mg^{2+} and Fe^{2+} ions were added. Veblen and Ferry (1983) examined the partially chloritized biotite described by Ferry (1979) using transmission electron microscopy. They showed that "alteration to chlorite proceeded by a process in which brucite-like layers replaced TOT mica layers", with a consequential volume loss of 30%. Although this volume change is somewhat greater than the change calculated from chemical data of 18% (after allowance for sphene), Veblen and Ferry found no evidence for the volume increasing mechanism they also

considered; viz. that extra brucite-like layers are inserted into the biotite interlayer. Olives Baños and Amouric (1984) have also used TEM to investigate the chloritization of metamorphic biotite. They conclude that the process is essentially the replacement of the potassium plane by a brucite-like sheet, in contrast to Veblen and Ferry's dominant mechanism.

Studies based on mineral chemistry and optically visible (> 1 μm) textures alone cannot characterize a reaction sufficiently to be unequivocal. Sub-micron-sized gaps or inclusions are not discernible with a light microscope, but they may be important factors when comparing volume relations between primary and pseudomorphing minerals. Furthermore, the proposition that a whole rock sample has experienced chemical gains and losses needs to be supported by comparative chemical analyses of altered and unaltered material.

Complete chemical analyses of granite samples from plutons of southeastern Australia (Beams, 1980) provide a firm data base on which to establish the nature of the chemical reactions in alteration processes. Two plutons from the Bega Batholith (Beams, 1980), the Kameruka and Quaama (rhymes with "warmer") granodiorites contain biotite sporadically altered to chlorite. In the Kameruka pluton biotite is the only primary Mg–Fe silicate, whereas the Quaama also contains amphibole. Beams has established that for these granites the variation in major element chemistry between unaltered samples of one pluton is completely deter-

mined by the initial granite-forming process. Therefore, any later reactions that introduce or remove elements can be detected as a deviation from the well-defined primary inter-element relations provided such changes amount to more than about 10% of the element abundance; in the case of MgO, about 0.2 wt. %. Whole rock analyses of granitic suites therefore can detect external gains and losses during late-stage chloritization. On the other hand, internal, or "within sample" elemental mobility can be partly defined in the Kameruka pluton, because biotite is the only primary (Mg, Fe)-silicate, and chlorite is the only secondary Mg-silicate. Therefore if magnesium is not gained or lost from the whole rock, the biotite–chlorite reaction must be Mg-conservative. These considerations form the chemical framework of the present study.

In this and other studies of the biotite–chlorite reaction, the reaction products appear in thin section to occupy all of the original biotite volume. Parry and Downey considered the possibility that "biotite is replaced by an equivalent volume of chlorite", although they also state that sphene is an alteration product. We have used transmission and scanning electron microscopy to examine the textural relations between the minerals and to provide the structural framework of this study.

Sample and methods

The Kameruka and Quaama plutons of the Bega Batholith of southeastern Australia have been included in BSc theses of the Australian National University by Lesh (1975), Beams (1975), Percival (1975) and Banfield (1981), and in a Doctoral thesis by Beams (1980). These studies have revealed a strong coherent inter-element relationship for all plutons of the Bega Batholith. In particular, Harker diagrams show consistently linear relationships between SiO_2 and major and trace elements (for example, Fig. 1) which have been interpreted following White and Chappell (1977) to result from mixing of melt and residual lower crustal material of originally igneous, or I-type, origin.

Although all 339 analyses of Bega Batholith rocks have been made on selected unweathered samples, the Kameruka and Quaama rocks show varying degrees of chloritization of the biotite. Examination of whole rock analyses shows close linear correlations between all elements except hydrogen. The water content ranges between 0.7% and 1.4%, with the more chloritized samples having the higher water content. No other element correlates with water content, although among major elements involved in the biotite–chlorite reaction, only Mg and K might be expected to show detectable change. Except for water, we conclude that the chloritization process was isochemical on the scale of the analytical sample (50 kg).

The Kameruka granodiorite contains large (50 mm) K-feldspar phenocrysts, with plagioclase, quartz and biotite, as well as accessory zircon, allanite, apatite and magnetite. The Quaama granodiorite contains prominent (up to 15 mm) sieve-textured plagioclase crystals, variable amounts of K-feldspar, euhedral amphibole, biotite, and quartz with accessory allanite, zircon, sphene, apatite, hydrogarnet, prehnite, and magnetite, and traces of pyrite and chalcopyrite.

Examples of the biotite–chlorite reaction were selected from optical thin sections. Energy dispersive electron microprobe analyses were made of many partially altered biotites from three localities. Specimens for electron microscopy were thinned by Ar-ion
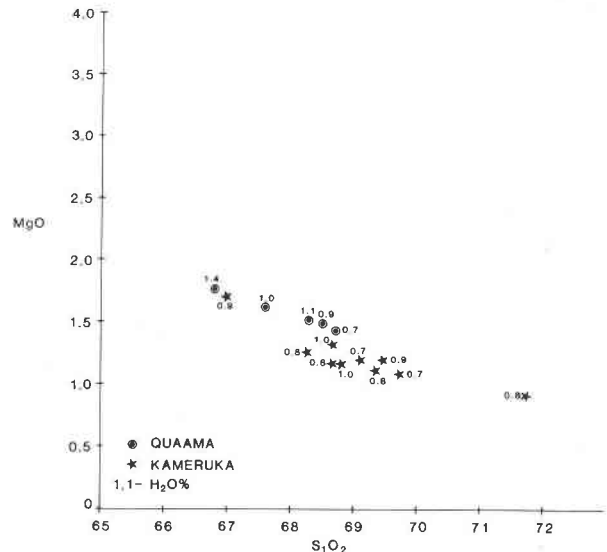

Fig. 1. MgO vs. SiO_2 for the Quaama (circles) and Kameruka (stars) plutons. Whole rock H_2O^+ figures are written beside each analysis point.

bombardment at 5 kV and examined in JEOL 100CX and JEOL 200CX Transmission Electron Microscopes. Ferrous iron, water, and density were determined only from a fourth analysed sample not examined by electron microscopy (AB333, Banfield, 1981).

Single crystal X-ray precession photographs, and Debye-Scherrer powder photographs show both 1M and $2M_1$ biotite, and that the chlorite is dominantly the IIb polytype. Electron diffraction patterns of the chlorite are extensively streaked parallel to c^*, indicating considerably stacking irregularity, and high resolution images confirm this. The cell parameters are: for biotite-1M $a = 5.367(6)$Å, $b = 9.273(7)$Å, $c = 10.238(7)$Å, $\beta = 99.97(16)°$, for chlorite $a = 5.360(3)$Å, $b = 9.286(4)$Å, $c = 14.258(8)$Å, $\beta = 97.18(3)°$. Walshe (pers. comm.) has estimated the alteration temperature of this assemblage at 338°C (assuming 1 kbar pressure), using the chlorite solid-solution model.

Alteration

Light microscopy

At low magnifications, the early stage of biotite alteration (i.e., when only 10% or so of the biotite is altered) appears to be pseudomorphic, or a constant volume process. Examination of completely altered biotites, however, shows in addition to biotite and its initial inclusions of sphene, apatite, zircon, and magnetite, newly formed sphene, epidote, probably new quartz, and small opaque grains, which might be new magnetite. These new inclusions may total 20% of the replaced biotite. Alteration of biotite is accompanied by sericitization of the andesine plagioclase, and it is common for a crystal of biotite to be more altered where it abuts a plagioclase than where it touches quartz or K-feldspar. These observations strongly suggest the coupled reaction: biotite + plagioclase → chlorite + epidote + sphene + muscovite. For this reaction to occur, K^+ and Ca^{++} must exchange between the biotite
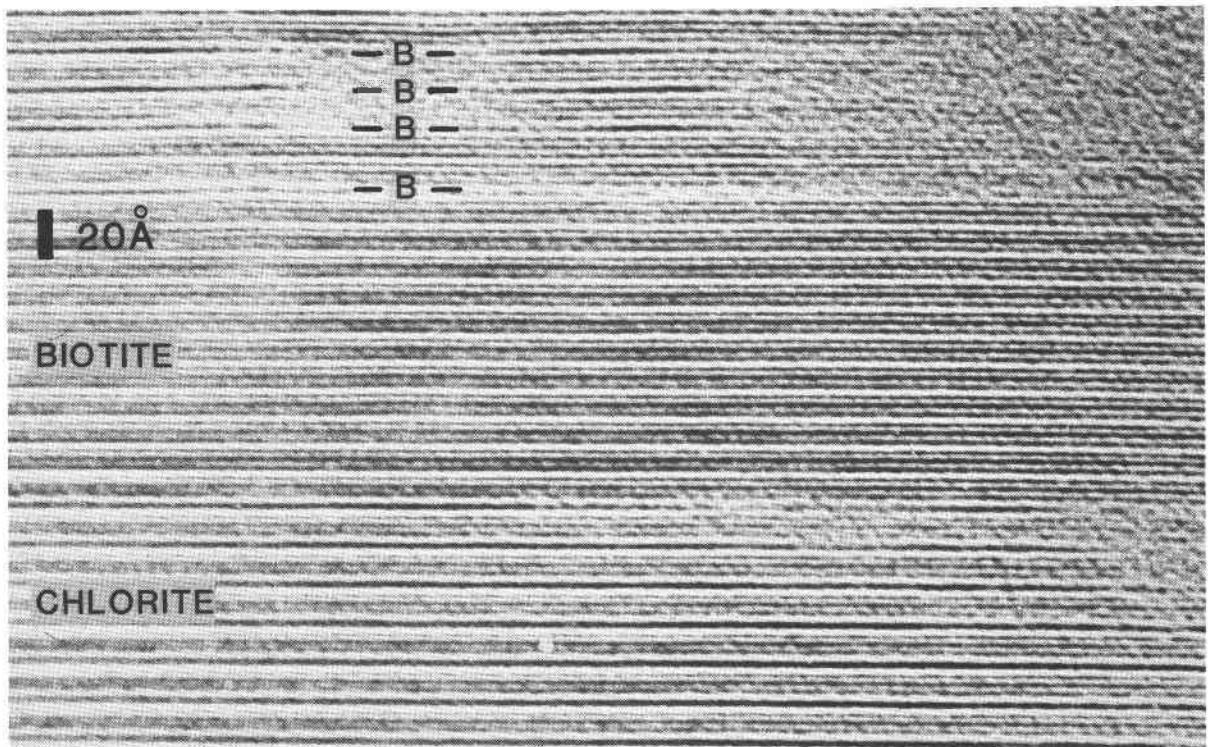
Fig. 2. Parallel intergrowths of biotite and chlorite, showing sequences of both structures, and occasional intercalation of brucite-like sheets (B) between the talc-like layers of biotite.

and plagioclase, presumably diffusing through the hydrous fluid responsible for the alteration.

Electron microscopy

Transmission electron microscopy (TEM) reveals that the interfingering of biotite with chlorite visible in the optical microscope extends at all scales down to single layer interstratification (Fig. 2). Once initiated, the change of a biotite layer to chlorite appears to run right along the layer before the next biotite layer alters, thus making it difficult to establish a direct volume relation between the two phases. The existence of splits and gaps in wider (<10 unit cells) chlorite bands points to a small volume loss on alteration (Fig. 3).

The first indication of alteration in biotite is the appearance of a single terminating talc-like layer (edge defect), followed by a 500Å long wedge-shaped gap between the flanking talc-like layers (Fig. 4). Edge defects without the wide gap are also found and such defects are presumably the initial focus for alteration. In a slightly later stage of development, the talc-like layer extends its octahedral sheet into what has become the chlorite interlayer, i.e., a biotite layer has lost its silica tetrahedra and K ions and become a brucite-like sheet (Figs 5, 6, 7). This mechanism was also described by Veblen and Ferry (1982) as their mechanism 2 (Fig. 8).

In other examples, a brucite-like sheet appears between

two talc-like layers and the biotite on either side is distorted to make space for the extra brucite (Figs 6, 7) (Veblen and Ferry's mechanism 1, Fig. 8). It is possible that such extra brucite-like sheets represent edge defects with the terminating TOT layer stripped of its tetrahedra in the same way as previously described. If the angular misfit between biotite and chlorite layers of Figure 7 represents an original low-angle grain boundary, edge dislocations would be expected and the images of terminating brucite-like layers might be tetrahedrally stripped biotite layers. On the other hand Figure 6 shows an image of two adjacent brucite-like sheets (marked '?'), at least one of which must have been added between original biotite layers. In the electron micrographs of the Quaama and Kameruka alteration, edge dislocations are extremely rare in fresh biotite, whereas terminating (or initiating) brucite-like sheets are common in biotite–chlorite intergrowths, and we conclude, as do Olives Baños and Amouric, that this mechanism (1) does take place. Thus, both contraction ($2 \times 10Å \rightarrow 14Å$) and expansion ($10Å \rightarrow 14Å$) occur, but overall a volume loss results, and as the reaction proceeds, wider cracks and gaps appear, most commonly between extensive regions of unaltered biotite on one side, and heavily chloritized biotite on the other. The material in these gaps appears amorphous, however it may be that it is more subject to electron beam damage than the biotite or chlorite. There is an indication in such regions that biotite strips are dissolved, for narrow
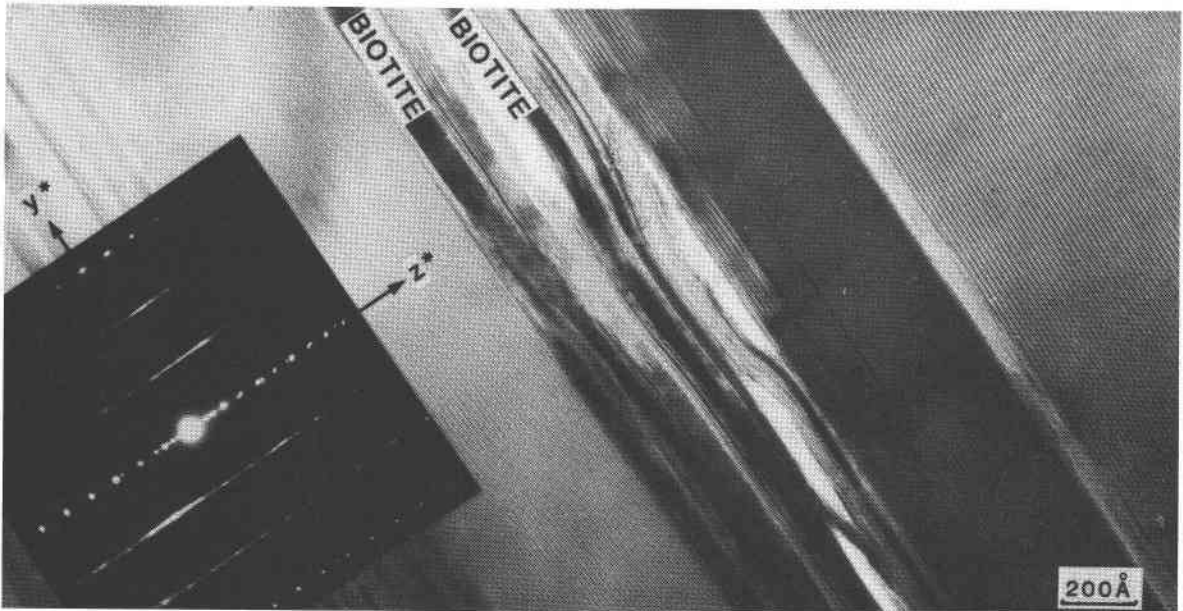
Fig. 3. Extensive areas of chlorite with remnant buckled biotite. Volume loss amounts to 3% over the photograph.

(50–100Å) needle-shaped fragments of biotite surrounded by structureless material are interleaved with chlorite (Fig. 9).

Sphene inclusions in chlorite have been identified by their diffraction pattern. These crystals are oriented with (110) parallel to the biotite–chlorite (001). They do not thin under Ar-ion bombardment as fast as the layer silicates, and are generally too thick to identify if the surrounding material is thin enough to be electron transparent. Under scanning electron microscopy, sphene crystals are visible ranging in size from 20 μm to the limit of resolution ($\sim$0.1 μm) of the X-ray elemental scan technique (Fig. 10). Epi-
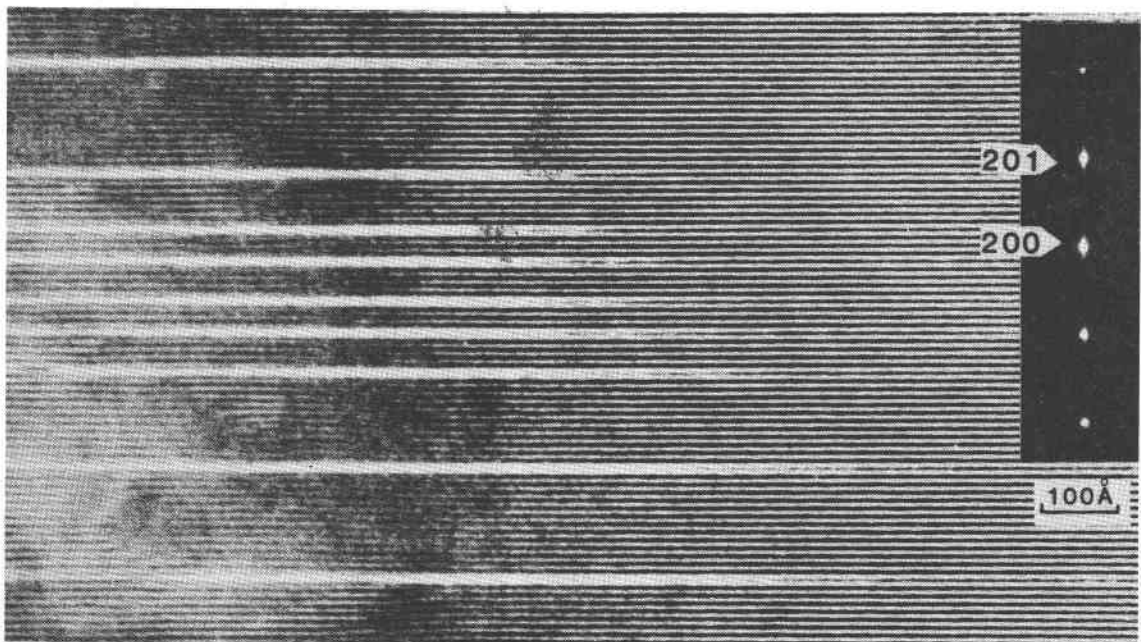

Fig. 4. Single layer defects in biotite. The mica closes back to 10Å at the left of each defect. Diffraction pattern shows streaking parallel to $\mathbf{c}^*$ in $k = 3n$ rows caused by the random changes in layer spacings.
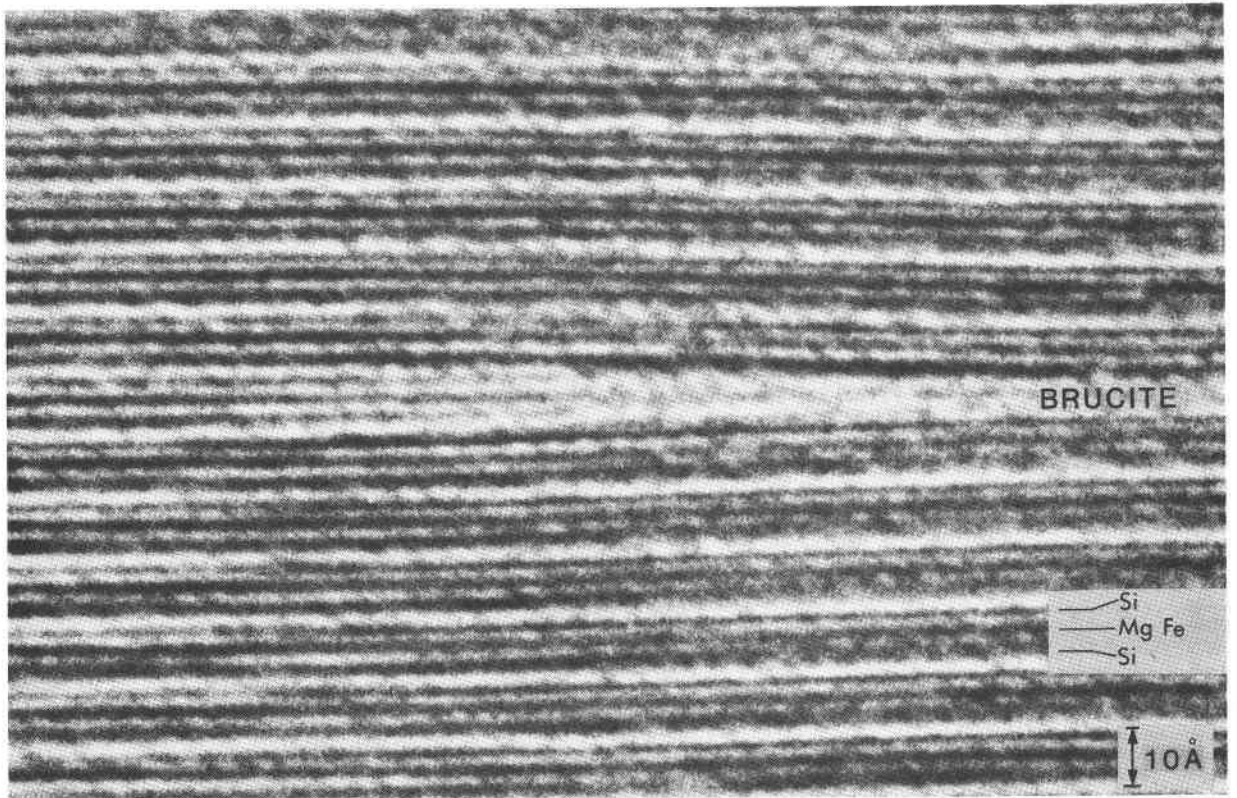
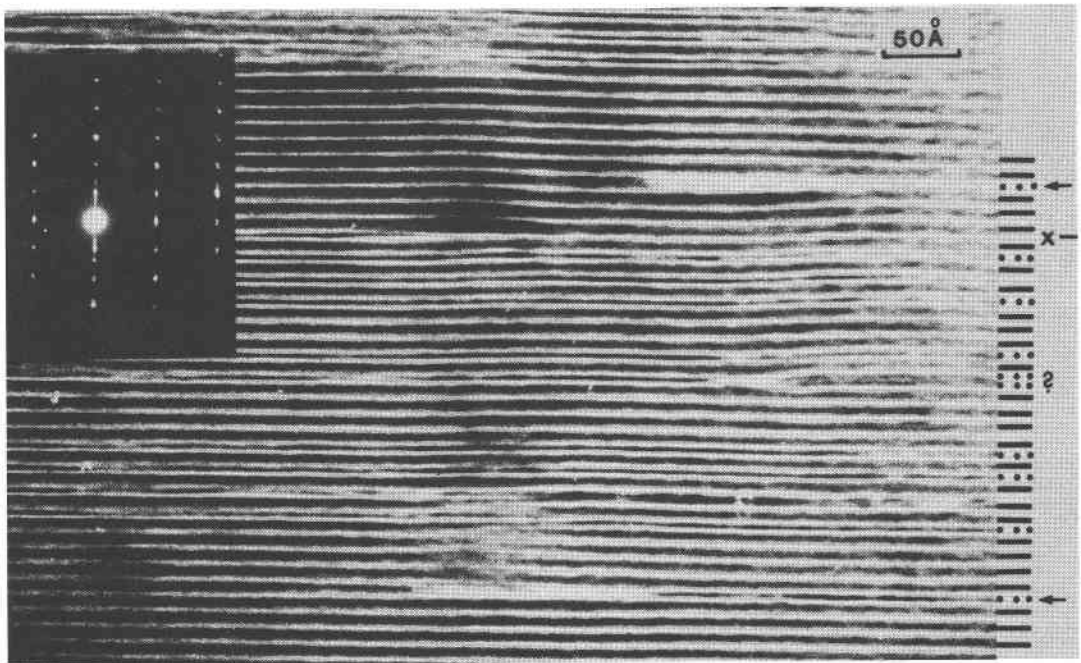Fig. 5. Production of a brucite-like sheet by loss of the tetrahedral sheets from a biotite 2 : 1 layer.

Fig. 6. Intergrown biotite and chlorite layers. Brucite-like sheets are indicated at the right by dots, talc layers by a line. Reduction of a talc layer to brucite is shown at arrows, the development of an extra brucite between talc is marked by the cross, and perhaps two extra brucite-like sheets by the query.
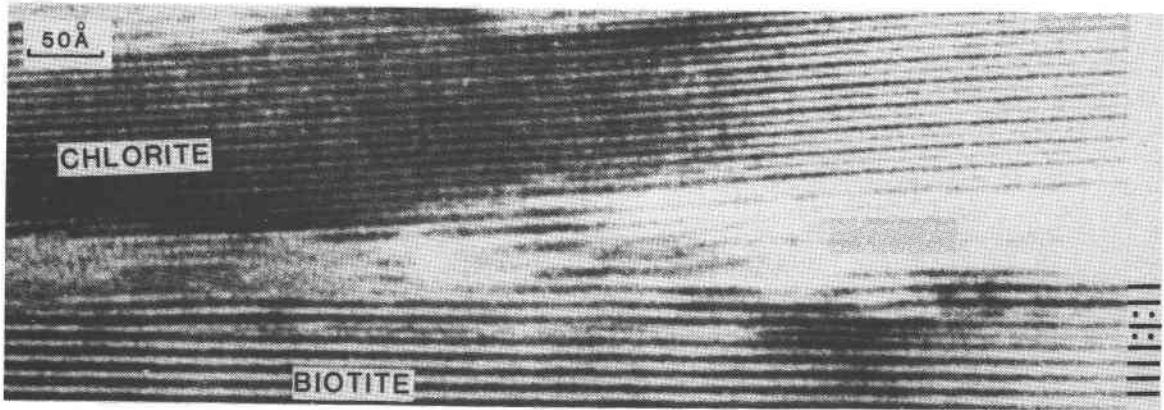
Fig. 7. Boundary between biotite and chlorite. Chlorite formation is shown as the insertion of brucite-like sheets (dotted on right) between 2:1 talc-like layers (lined on right).

dote has not been detected by TEM. Regions of high Ca and low Ti and P are seen in SEM and are interpreted as epidote.

Chemistry

Average electron microprobe analyses for chlorite and biotite from three localities are presented in Table 1. The Fe^{3+}/Fe^{2+} ratio of 0.2 was measured by spectrophotometry from a fourth sample (taken from the Quaama granodiorite), and there is little difference between this ratio in the biotite and chlorite (biotite:0.20, chlorite:0.18). The structural formulae indicate that the biotite is essentially free of octahedral Al, and that the tetrahedral sheets of biotite and chlorite have a similar Si:Al ratio. The six paired analyses of Ferry (1981) show the same

similarity between tetrahedral sheets, however there is more variation in Parry and Downey's data (1982). The chemical results confirm the electron microscope observation that the talc-like layer of the chlorite is inherited directly from the biotite.

Parry and Downey noticed that chlorite from more altered biotite had a higher Mg content than chlorite from less altered biotite. Figure 11 shows some individual analyses for biotite–chlorite pairs from the present study; the parallelism of the lines connecting analyses from the same crystal indicates that the biotite composition is the main factor in determining chlorite composition in this reaction. Major differences between biotite and its chlorite reaction product are the high Al content of the chlorite octahedral sheet, and the total loss of Ti from biotite. Thus although
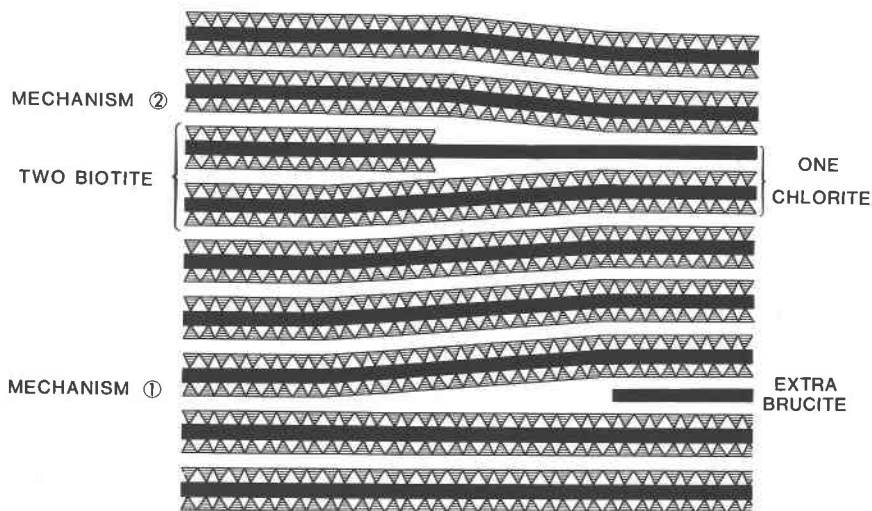

Fig. 8. Schematic diagram of the two mechanisms considered for the development of chlorite from biotite, following Veblen and Ferry. In mechanism 1, a brucite-like sheet replaces the K-interlayer of biotite; in mechanism 2, the loss of tetrahedra from one biotite layer reduces it to a brucite-like layer, so that 2 biotites become one chlorite.
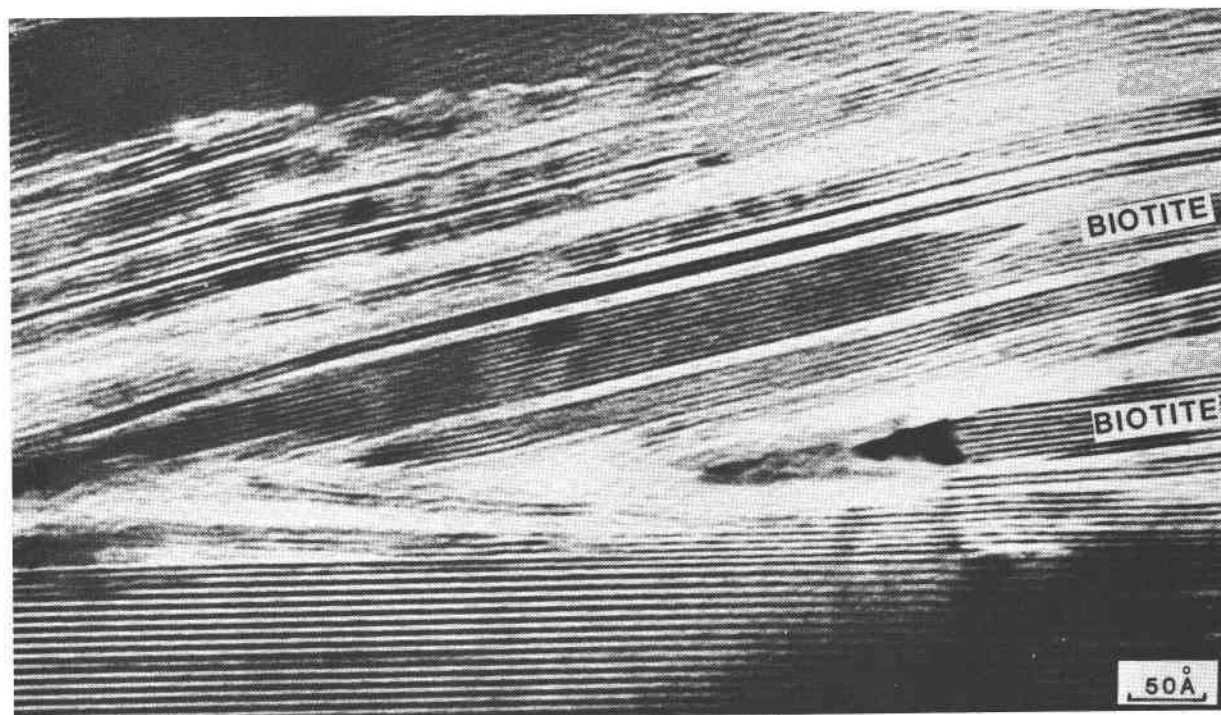
Fig. 9. Remnant biotite in chlorite. Dissolution of biotite is suggested by the tapering shape and the presence of low contrast, possibly amorphous, material.

the tetrahedral sheets appear to be inherited intact, there is free element exchange in the octahedral site.

The absence of a source or sink for Mg in the Kameruka granodiorite external to the biotite–chlorite mixture is a strong indication that the reaction is Mg-conservative. The similarity of the reaction in the Quaama granodiorite, and
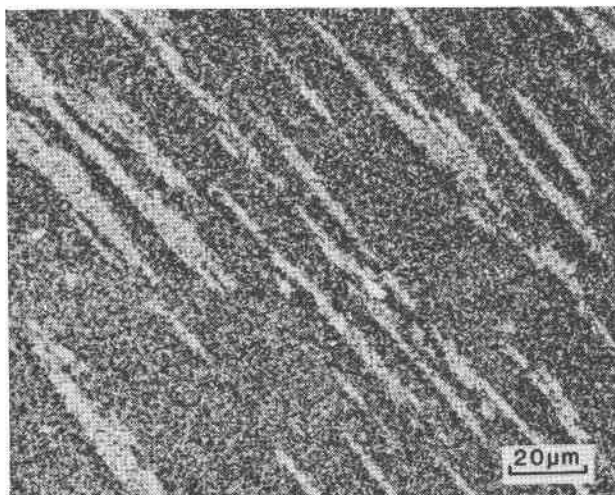

Fig. 10. Narrow sphene crystals (ligher shade) in chlorite (SEM of polished surface).

the unaltered appearance of the amphiboles in this pluton suggest a similar process occurs there also. The Ti lost from biotite is presumed to be incorporated into sphene, and the decrease in Fe:Mg and Al:Mg ratios from biotite to chlorite suggests that the Fe and Al in the epidote is derived from the alteration of biotite. On this basis, the reaction for the average of samples 1–3 can be written (in numbers of unit cells for crystalline reactants), 1 biotite + 0.21 anorthite + 1.64 H_2O + 1.46H^+ + 0.08 $O_2 \rightarrow$ 0.46 chlorite + 0.11 sphene + 0.10 epidote + 0.56 muscovite + 0.63 quartz + 0.02 magnetite + 1.46 K^+.

The volume of the biotite, 501$Å^3$, is equal to that of the reaction products (excluding muscovite presumed to be within plagioclase).

The overall reaction as summarized in Table 2 only requires the addition of Ca^{2+}, H_2O and H^+ to the biotite, and the loss of K^+. We have not made a detailed examination of the altered plagioclase, and we cannot say what effect the albite component has on that part of the reaction, or whether muscovite is an actual reaction product, or if epidote is present in the altered cores of the plagioclase crystals. In the latter case, iron for epidote may be released from the altering biotite, instead of being fixed in magnetite, with a consequent volume loss of about 2%. The crinkles in chlorite seen in the electron micrographs can readily account for such a small volume loss.

These volume relations were checked by point-counting regions of completely altered biotite. Sphene is a primary

Table 1. Chemical analyses and structural formulae of biotites and chlorites

	43499		45131		45132	
	biotite	chlorite	biotite	chlorite	biotite	chlorite
SiO_2	35.69	25.83	35.04	24.58	35.49	25.23
TiO_2	3.64	0.12	3.75	0.23	3.77	0.13
Al_2O_3	14.23	19.06	14.65	19.27	14.16	18.29
FeO	20.84	24.11	22.76	26.79	31.92	25.64
MnO	0.31	0.67	0.30	0.62	0.30	0.61
MgO	11.39	16.11	8.86	13.68	9.56	14.93
CaO	0.10	0.02	0.10	0.10	0.00	0.03
K_2O	9.65	0.12	9.49	0.17	9.66	0.08
Na_2O	0.09	0.25	0.14	0.22	0.16	0.25
Sum	94.94	86.29	95.09	85.84	95.02	85.19
Si	2.74	2.73	2.71	2.65	2.74	2.72
Al	1.26	1.27	1.29	1.35	1.26	1.28
Ti	0.21	0.01	0.22	0.02	0.22	0.01
Al	0.03	1.10	0.04	1.10	0.03	1.05
Fe^{3+}	0.27	0.43	0.29	0.49	0.28	0.46
Fe^{2+}	1.07	1.70	1.18	1.95	1.13	1.85
Mn	0.02	0.06	0.02	0.06	0.02	0.06
Mg	1.19	2.53	1.02	2.20	1.10	2.40
Ca	0.01	0.00	0.01	0.01	0.00	0.00
K	0.95	0.02	0.94	0.02	0.95	0.01
Na	0.01	0.05	0.02	0.05	0.02	0.05

43499   : Quaama

45121, 2 : Kameruka

biotite structural formulae calculated to +22

chlorite structural formulae calculated to +28

Fig. 11. MgO vs. FeO for biotite and chlorite analyses from individual crystals.

constituent of the rock, and occurs within biotite; only sphene present in chlorite as thin (<5 μm) lamellae parallel to the chlorite cleavage was counted as secondary sphene. The results are listed in Table 3, and offer support for the reaction proposed. A small amount of quartz (3.5%) was also seen in chlorite, mainly at the grain edges. The difficulty of distinguishing secondary from primary quartz makes measurement meaningless, and the point count has been recast to 100% chlorite plus epidote plus sphene.

Mechanism

The observations we have described for this biotite–chlorite reaction suggest a sequence of alteration steps. Water in the granite provides hydrogen ions which diffuse along the biotite interlayer and substitute for K^+. As K^+ diffuses out, the H^+ attached to the tetrahedral sheet weakens the Si–O or Al–O bonds, initiating dissolution of the talc-like layer. This immediately widens the interlayer region, increasing the accessibility to water and accelerating the alteration of that talc-like layer. By such a mechanism two biotites may become one chlorite, with a large (30%) volume loss. Continuation of this process ultimately produces wide gaps between chlorite–biotite sequences, into which some of the released cations migrate, where they combine with Ca^{2+} diffusing in from plagioclase to form
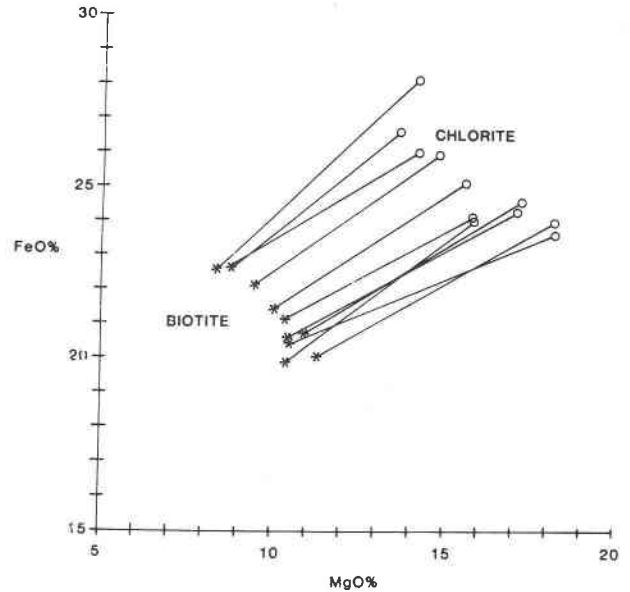
sphene and epidote. At the same time, octahedral cations and anions from completely dissolved talc-like layers, reconstitute into a brucite-like sheet between pairs of unaltered talc-like layers, with a marked volume increase (10 → 14Å). This reaction probably does not occur until the initial alteration has made space available. Veblen and Ferry also note that their mechanism 1 (2 biotite → 1 chlorite) involves a 30% volume loss, but regard the difference between this and the chemically derived volume loss of 18% as slight. They point out that a process involving 85% of their mechanism 2 with 15% mechanism 1 would match the chemically derived volume equation. Olives Baños and Amouric regard terminating brucite-like layers as evidence for mechanism 1, the "brucitization of the interlayer". Such features could equally result from the reduction of a terminating biotite layer to a brucite-like layer (mechanism 2 at an edge dislocation), and the observation alone cannot prove either mechanism.

The overall result of the reaction studied here is that 2 biotites become 0.92 chlorite, which suggests that mecha-

Table 2. Element loss (atoms/biotite structural formula) when 1 biotite → N chlorite at constant Mg

Sample	N	K	Ti	Mn	ΣFe	Al	Si
1	0.47	0.95	0.21	0.01	0.34	0.19	1.46
2	0.46	0.93	0.21	0.01	0.33	0.19	1.48
3	0.46	0.95	0.22	0.01	0.35	0.22	1.49

Table 3. Chlorite : sphene : epidote ratios

	Point count	Calculated from reaction
chlorite	80	79
sphene	11	10
epidote	9	11

nism 2 is dominant. The drive for this reaction is the introduction of H^+ ions, whereas the controlling factor appears to be the available space. Only K^+ diffuses out, Ti, Si, Al, Fe and Mg, though having very different solubilities and diffusion characteristics, all remain within the original biotite outline.

The biotite–chlorite reaction also provides a good example of structural inheritance in an alteration process. The a and b cell parameters of the two layer silicates are within 0.1%, allowing strain-free fit. The biotite 2:1 layer is passed complete to the chlorite although with octahedral cation re-equilibration, predominantly $3Ti^{4+} \rightarrow 4Al^{3+}$. The tetrahedral sheet is transferred intact.

Acknowledgments

References

Banfield, J. F. (1981) Geology of the Murrabrine Mountain area. BSc (Hons) Thesis, Australian National University, Canberra.

Beams, S. D. (1975) The geology and geochemistry of the Wyndham Whipstick area N.S.W. BSc (Hons) Thesis, Australian National University, Canberra.

Beams, S. D. (1980) Magmatic evolution of the southeast Lachlan Fold Belt. PhD Thesis, La Trobe University, Melbourne.

Eggleton, R. A. (1983) The formation of iddingsite rims on olivine: a transmission electron microscope study. Clays and Clay Minerals, 32, 1–11.

Eggleton, R. A. and Boland, J. N. (1982) Weathering of enstatite to talc through a sequence of transitional phases. Clays and Clay Minerals, 30, 11–20.

Ferry, J. M. (1979) Reaction mechanisms, physical conditions and mass transfer during hydrothermal alteration of mica and feldspar in granitic rocks from south-central Maine, U.S.A. Contributions to Mineralogy and Petrology, 68, 125–139.

Lesh, R. H. (1975) The geology and geochemistry of the Candelo-Bega region, New South Wales. BSc (Hons) Thesis, Australian National University, Canberra.

Loughnan, F. C. (1969) Chemical Weathering of Silicate Minerals. Elsevier, New York.

Olives Baños, Juan and Amouric, M. (1984) Biotite chloritization by interlayer brucitization as seen by HRTEM. American Mineralogist, 69, 869–871.

Parry, W. T. and Downey, L. M. (1982) Geochemistry of hydrothermal chlorite replacing igneous biotite. Clays and Clay Minerals, 30, 81–90.

Percival, P. J. (1975) The geology and geochemistry of the Cobargo area, New South Wales. BSc Field Mapping Report, Australian National University, Canberra.

Veblen, D. R. and Buseck, P. R. (1980) Microstructures and reaction mechanisms in biopyriboles. American Mineralogist, 65, 599–623.

Veblen, D. R. and Ferry, J. M. (1983) A TEM study of the biotite-chlorite reaction and comparison with petrologic observations. American Mineralogist, 68, 1160–1168.

White, A. J. R. and Chappell, B. W. (1977) Ultrametamorphism and granitoid genesis. Tectonophysics, 43, 7–22.